◆ Human Brain Mapping 8:235–244(1999) ◆

Determination of Drug-Induced Changes in Functional MRI Signal Using a Pharmacokinetic Model

Alan S. Bloom,[1]* Raymond G. Hoffmann,[2] Scott A. Fuller,[3] John Pankiewicz,[3] Harold H. Harsch,[3] and Elliot A. Stein[1,3,4]

[1]*Department of Pharmacology and Toxicology, Medical College of Wisconsin, Milwaukee, Wisconsin*
[2]*Department of Biostatistics, Medical College of Wisconsin, Milwaukee, Wisconsin*
[3]*Department of Psychiatry and Mental Health Science, Medical College of Wisconsin, Milwaukee, Wisconsin*
[4]*Biophysics Research Institute, Medical College of Wisconsin, Milwaukee, Wisconsin*

Abstract: As the applications of functional magnetic resonance imaging (fMRI) expand, there is a need for the development of new strategies for data extraction and analysis that do not require the presentation of stimuli in a repeated on / off pattern. A description and evaluation of a method and computer algorithm for the detection and analysis of brain activation patterns following acute drug administration using fMRI are presented. A waveform analysis protocol (WAP) input function has been developed that is based upon the single-dose pharmacokinetics of a drug of interest. As a result of this analysis, regional brain activation can be characterized by its localization and intensity of activation, onset of action, time to peak effect, and duration of action. A global statistical test for significant drug effects based upon the probability of a voxel being activated by a saline vehicle injection is applied to grouped data on a voxel by voxel basis. Representative data are presented using nicotine as a prototypical agent. Using this method, statistically significant drug-induced brain activation has been identified in several key cortical and subcortical brain regions. *Hum Brain Mapping 8:235–244, 1999.* © 1999 Wiley-Liss, Inc.

Key words: nicotine; brain; clustering; magnetic resonance imaging; pharmacology

INTRODUCTION

Functional magnetic resonance imaging (fMRI) is a method for measuring and mapping brain activation patterns in response to sensory stimulation, motor activity, or cognitive task performance. One of the most commonly used fMRI methods is based upon changes in blood flow and delivery of oxygen following neuronal activation. Specifically, the blood oxygenation level dependent (BOLD) signal is derived from the long-standing observation of the tight coupling between neuronal activity, localized blood flow, oxygen consumption, and glucose utilization [Sokoloff, 1977]. An increase in blood flow and hemoglobin oxygenation occurs at the capillary level in metabolically active brain tissue to such an extent that the relative extraction of oxygen with respect to blood flow delivery is actually less in spite of increased metabolic demand. Thus the relative increase in oxyhemoglobin

Contract grant sponsor: US PHS; Contract grant number: DA09465; Contract grant sponsor: GCRC; Contract grant number RR00058.

*Correspondence to: Alan S. Bloom, Department of Pharmacology and Toxicology, Medical College of Wisconsin, 8701 Watertown Plank Road, Milwaukee, WI 53226. abloom@mcw.edu

Received for publication 17 November 1998; accepted 18 June 1999

to deoxyhemoglobin leads to decreased spin dephasing and increased MRI signal in the active region [Ogawa et al. 1992a,b, 1993]. Previous fMRI studies [Bandettini et al., 1993; Binder et al., 1994; DeYoe et al., 1996] have examined the signal changes occurring between an ''active'' and ''resting'' state using alternating repetitive presentations of sensory stimuli, cognitive or motor tasks interspersed with a no stimulus period. This repetitive on-off stimulation pattern has been generally used since the signal change in the BOLD response is quite small and variable with signal changes in the range of 1–3%. One of the most common methods to identify regions of brain activation using fMRI is based upon a cross-correlation statistic calculated against an alternating on/off input function that exactly matches the temporal pattern of the stimulus or task [Bandettini et al., 1993].

In addition to sensory, motor, and cognitive tasks, fMRI appears to be a valuable tool to study the effects of drug action in the brain. However, how to extract specific drug-induced effects from fMRI signals is not readily apparent. This is particularly important in determining the specific CNS effects of a drug from nonspecific changes due to the experimental milieu. Further, the use of cross-correlation analysis is inappropriate for acute drug studies since drug injections and their response input functions tend to be of relatively long duration and thus do not permit rapidly alternating periods of activation and rest as do motor, cognitive, and sensory tasks. The power of cross-correlation analysis increases with the number of on/off reversals in a data set and requires at least three to five periods for adequate statistical sensitivity [Bandettini et al., 1993]. Only one published fMRI study examining the effects of an acute drug injection on brain activation has appeared [Breiter et al., 1997]. The analysis used in that study simply compared all pre-injection time points with all time points after the injection, losing much of the temporal information available from fMRI.

A drug's pharmacokinetics or the time-related changes in drug concentration within the bloodstream or other compartments of the body are measurable, predictable, and known for most commonly used drugs [Hardman and Limbird, 1996]. As such, we propose using as an alternative means of signal detection, an input function based upon the single dose pharmacokinetics of a drug of interest. Several assumptions must be made to merge pharmacokinetics with fMRI signal processing. First, it is posited that the concentration of a drug in the brain is directly related to its concentration in the circulation. This is particularly true after an acute administration of lipophilic, short-acting drugs such as nicotine and cocaine. This relationship is diminished at longer times after drug administration, when significant drug redistribution from the brain has occurred. These drugs are ideal prototypes for this type of analysis since when administered by the iv route, they have a rapid onset and a relatively short duration of action. The total time of drug action in a single dose experiment is well within the range of a single fMRI run, generally 10–20 min.

With iv administration, the pharmacokinetics of these drugs are characterized by a rapid distribution phase where they distribute throughout the body, including the brain, proportional to the organ's blood flow. Thus brain concentration of drug is thought to reflect blood drug concentration during this early distribution phase. This is followed by an elimination phase where the drug first leaves the brain by redistribution and/or metabolism and is ultimately metabolized and excreted from the body. For most drugs, the elimination follows first-order kinetics characterized by an exponential decline in circulating blood concentrations of the drug [Hardman and Limbird, 1996].

Second, it is assumed that brain activity, as reflected by changes in fMRI BOLD signal over its dynamic range, is directly driven by brain drug concentration. Finally, it is assumed that the drug is acting upon neuronal elements and not indirectly via actions on the cerebral vasculature or upon peripheral cardiovascular variables. These factors are discussed below.

The signal detection and extraction procedure described below for the analysis of drug effects using fMRI is predicated on an understanding of these pharmacokinetic properties. A description of a waveform detection procedure based upon a pharmacokinetic algorithm and its application to detect changes in regional brain activation following acute nicotine administration is presented.

MATERIALS AND METHODS

Drug administration and fMRI

All experiments were performed on a GE 1.5 Tesla Signa scanner. A 30.5 cm ID three axis, balanced torque, local gradient coil designed and built specifically for rapid gradient switching [Wong et al., 1992] replaced the standard Signa gradient coil. A shielded quadrature elliptical endcapped transmit/receive birdcage RF coil, inserted inside the gradient coil, was used to obtain high quality images throughout the total brain volume. A blipped, gradient-echo, echo-planar image (EPI) pulse sequence (TE = 40 ms) with an interscan resolution (TR) of 6 sec was used to acquire

eight contiguous 8 mm axial slices. A 124 slice set of 1.1 mm spoiled GRASS images was obtained to place individual subjects' data into common stereotactic space and allow for the 3D display of the functional data set.

After informed consent was obtained, both saline vehicle and nicotine were administered to 15 experienced strongly righthanded cigarette smokers (mean age = 26 yr). Of these, 10 subjects also provided satisfactory movement free images after the nicotine injection. Heart rate was monitored using a pulse oximeter (In Vivo Systems). Subjects had an IV catheter inserted into the left arm for nicotine delivery. Catheter patency was maintained via a gravity-fed, 0.154 M saline solution infused at a rate of 60 ml/hr. Immediately preceding each drug injection, the IV line was allowed to run rapidly and saline vehicle or nicotine injected into a port close to the subjects arm. Drugs were administered over a 1-min period in a total volume of 10 ml, following a 4-min baseline scanning period. Scanning was continued for an additional 15 min after the completion of the injection. A nicotine dose of 1.5 mg and its saline vehicle were analyzed in the present example. This protocol was conducted under the approval of the Institutional Review Board of the Medical College of Wisconsin.

Waveform Analysis Protocol (WAP)

A program making use of our waveform analysis strategy (WAP) was written using the C language and is run with a graphical user interface. An idealized drug response fMRI waveform based upon our pharmacokinetic working hypothesis and the known pharmacokinetics of nicotine is shown in Figure 1. The model requires an input of a limited range of values to define relevant waveform parameters. These would be changed based upon the known and/or observed pharmacokinetics of other drug to be studies. Active voxels are detected using six criteria including time to peak effect, magnitude, and statistical significance of peak effect, slope of the rising phase of the response curve, time to decline back to 50% of peak, and the stability of the baseline period (baseline period range ≤11% of the mean range for all brain voxels, which was arbitrarily selected based on the magnitude of the peak drug response). The acceptable range for each parameter is determined from both the known and our previously measured [Stein et al., 1998] pharmacokinetics of nicotine, or another drug appropriate for study, and the observed physiological and behavioral effects in that study. The parameters used for iv nicotine are

A.

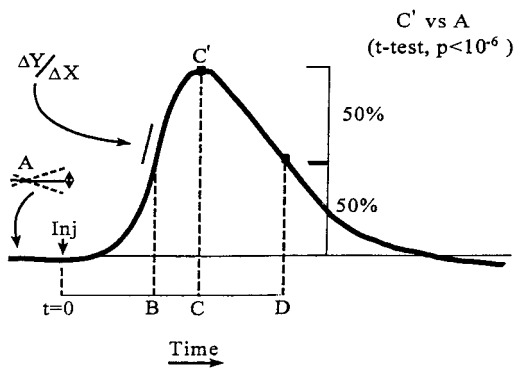

B.

PARAMETER	ACCEPTABLE RANGE
Time to Peak Response (t = 0 to C)	1 to 8 minutes after start of injection.
Peak Response (C')	≥ 0.5 % over baseline
Time for Response to Decline to 50% of Peak (t = 0 to D)	4 to 12 minutes after injection
Slope of Rising Phase of Response (ΔY/ΔX) at time B	0.5 to 5.0
t-test of peak height vs. baseline	$p \leq 10^{-6}$
Baseline Stability	Range of A ≤ 11% of mean range for all voxels in brain

Figure 1.

A. An idealized drug response fMRI waveform based upon a pharmacokinetic working hypothesis. The model requires an input of a limited range of values to define relevant waveform parameters. Specific parameters are defined from both the known pharmacokinetics of the drug and empirically modified following visual inspection specific waveform characteristics of the data. The waveform analysis parameters used for iv nicotine are shown in **B.**

shown in Figure 1. In order to be considered active, a voxel has to meet all criteria. An adjustment for the autocorrelation between successive observations is included to ensure a correct *P* value [Milliken and Johnson, 1992]. For our observed autocorrelation of 0.5, the correction factor is 1.8, i.e., the t-value is divided by 1.8 to correct for the autocorrelation. The effect of the autocorrelation between the baseline set of observations and the peak set of observations is minimized by making sure that there is a gap of at least three observations (for an autocorrelation of 0.5, this assures that the two groups are essentially independent, $P < 0.05$.)

Our analysis protocol is applied to every voxel within the brain to produce activation maps that can be displayed using any of the calculated waveform parameters. Activation maps and SPGR data sets from each subject are transformed into 3D proportionally

measured stereotaxic coordinates relative to the line between the anterior and posterior commissures (AC-PC line) as described by Talairach and Tournoux [1988] using the *A*nalysis of *F*unctional *N*euro*I*mages (AFNI) program [Cox, 1996]. In a typical experiment, saline vehicle and multiple doses of each drug (in this case nicotine) are administered to each subject. The WAP methodology is applied separately for each drug injection. The number of voxels activated by a saline injection is calculated for each subject using the same waveform parameters used for drug-induced activation and used as discussed below to calculate the statistical significance level of voxels activated by drug in the entire subject population.

Statistical theory and methodology for assessing drug effects in fMRI studies

Once activation maps are generated and placed into stereotaxic space, AFNI allows them to be added or averaged across all subjects in a treatment group. To address the question of which brain regions have been significantly activated (and by how much) by a given drug treatment, we use a model for the activation across persons that assumes each person has a different false positive rate determined by the saline infusion. The initial assumption is that each individual will have a potentially different rate, p_I, that a voxel will have the same temporal trajectory with a saline infusion as the response expected from the drug intervention

$$p_i = pr[\text{active voxel in individual i}|\text{saline infusion}] \quad (1)$$

Since each subject represents an independent measure, the number of individuals that have the same voxel activated should follow a binomial-like distribution.

If p_i were the same for each individual, the distribution would be binomial. Since the p_i may vary, it is a binomial distribution with a distribution on p. A flexible distribution that can be used to model the distribution of the p_i is the beta distribution:

$$pr(p_i = x) = \frac{x^{a-1}(1-x)^{\beta-1}}{B(\alpha, \beta)} \quad (2)$$

where,

$$B(\alpha, \beta) = \frac{\Gamma(\alpha)\Gamma(\beta)}{\Gamma(\alpha+\beta)} \quad (3)$$

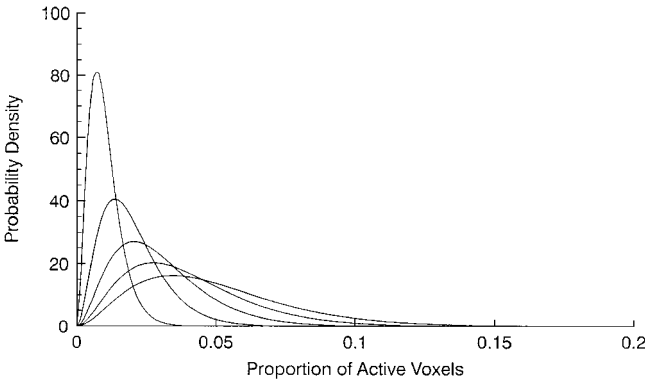

Figure 2.
Graphs of the beta distribution with mean probabilities (p_i) of 0.01, 0.015, 0.02, 0.03, and 0.05 (left to right, respectively) illustrate the ability of the beta distribution to flexibly model a wide variety of between subject variability.

and $\Gamma(.)$ is the gamma function [Evans et al., 1993]. Figure 2 shows how the beta distribution varies for a range of parameter values. The mode or highest value occurs at $(\alpha - 1)/(\alpha + \beta - 2)$. The graphs are obtained by fixing alpha at 3.0 and adjusting beta to shift the mode from 0.01–0.04 corresponding to proportions of active voxels in the control state.

Each p_I is estimated by the proportion of active voxels during the saline infusion. We estimated the parameters of the beta distribution by first using the sample mean, $\bar{x} = .0335$, and the sample variance, $s^2 = .0201$ to produce the moment estimates,

$$\hat{\alpha} = \bar{x}\left[\frac{\bar{x}(1-\bar{x})}{s^2} - 1\right], \quad (4)$$

and

$$\hat{\beta} = (1-\bar{x})\left[\frac{\bar{x}(1-\bar{x})}{s^2} - 1\right] \quad (5)$$

The moment estimates for alpha and beta, 2.648 and 76.323, respectively, were then used as starting values for the maximum likelihood equations [Evans et al., 1993] and iterated until convergence produced, alpha = 2.35 and beta = 66.64 for the maximum likelihood estimates. The composite distribution, the beta-binomial has the explicit probability density function

$$p[x = k \text{ individuals have an active voxel}|\text{n individuals}, \alpha \text{ and } \beta] = \binom{n}{x}\frac{B(\alpha + x, \beta + x)}{B(\alpha, \beta)} \quad (6)$$

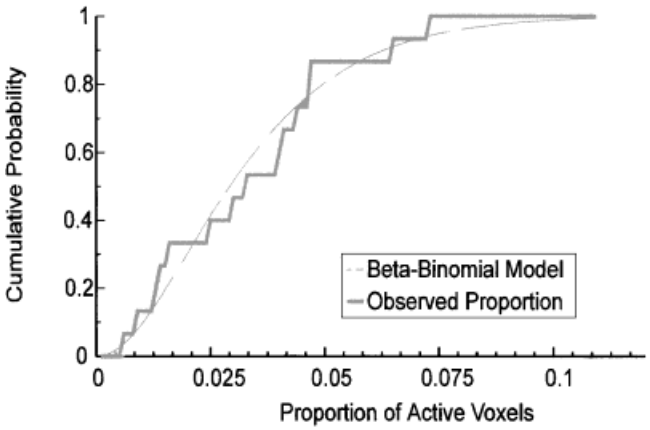

Figure 3.
A comparison of the observed cumulative distribution function with the beta distribution for saline, when α (2.35) and β (66.638) were determined by maximum likelihood (n = 15).

[Evans et al., 1993]. Thus the tail probabilities can be computed using the beta-binomial distribution as

$$p[x \geq k \text{ persons active} | \bar{p} \text{ and } n \text{ individuals}] = \sum_{x=k}^{n} \binom{n}{x} \frac{B(\alpha + x, \beta + x)}{B(\alpha, \beta)} \quad (7)$$

Using the saline data, we compared the observed cumulative distribution function with the beta distribution, with α and β determined by maximum likelihood (Fig. 3). This distribution is then used to develop a series of tables that enable the user to determine the number of subjects that must have a particular voxel active in order for it to be statistically different than saline at a previously chosen probability level (Table I). The table only depends upon the average proportion of voxels active during the saline infusion; it is not dependent upon the parameters of the WAP nor upon the pharmacokinetics of the drug being infused. A sample data set is presented in the next section.

Each voxel is tested separately against the null hypothesis of no activation. The operating point of the test (the balance between the specificity of the test—the ability to eliminate false positives—and the sensitivity of the test—the ability to detect true positives) can be tested with a saline infusion. The saline infusion produces activated voxels by chance alone, and the sensitivity of the test can be adjusted so that 5%, 1%, or 0.1% of the voxels are active in the control condition at the expense of the power to identify truly active voxels. The WAP criteria are adjusted so that the saline level exhibits a 1% or smaller random activation. Further reductions in the false positive rate can be achieved by reducing the % of saline false positives with more stringent criteria, e.g., by decreasing the probability of a false positive and / or by increasing the probability of a true positive with a clustering requirement for active voxels, which eliminates the random isolated voxel [Forman et al., 1995]. The investigator chooses the operating point depending upon the relative number of false positive voxels and the effect size.

RESULTS

In order to demonstrate the applicability of this waveform recognition algorithm and statistical methodology, we have applied it to a series of fMRI images acquired from subjects receiving iv nicotine while undergoing whole brain scanning. Representative raw fMRI data from a single 8 mm slice from one subject are shown in Figure 4. Drug-induced changes in fMRI signal were extracted using the WAP method described above with detection parameters determined from examination of each parameter in the subject population and their agreement with published reports of nicotine pharmacokinetics [Benowitz et al., 1990]. These values were consistent with our previously published nicotine plasma levels and behavioral effect time courses [Stein et al., 1998] and are listed in Figure 1 for the data illustrated.

Ten subjects successfully completed the study examining the effects of 1.5 mg nicotine and its saline vehicle. Other subjects' data were eliminated from the 1.5 mg nicotine group due to movement artifacts induced by the drug injection (5 subjects), but were movement free after saline and included in our saline probability data. Significant differences between the responses to saline and nicotine were found for total number of activated voxels and peak signal magnitude. The mean percentage of voxels within the brain that met the nicotine waveform recognition criteria after saline vehicle injection was 3.2% ± 0.6% (range 0.9–6.5%). This was significantly increased almost fourfold by 1.5 mg of nicotine to 11.1% ± 2.4% (range 3.0–31.8%). All subjects displayed an increased number of activated voxels after nicotine. The mean time to peak response after completion of injection was 3.4 ± 0.4 min. The mean fMRI signal response magnitude to nicotine was 2.3% ± 0.2% when compared to the baseline period and the mean time for the MRI signal intensity to return to 50% of peak was 5.7 ± 0.3 min after nicotine injection. These values agreed well with the time course for plasma nicotine levels and behavioral responses previously published by us [Stein et al.,

TABLE I. Critical values for the determination of significant voxel activation*

	Percent saline activated voxels									
Group Size	.005	.01	.02	.03	.04	.05	.075	.10	.15	.20
n = 8										
2	.0010	.0039	.014	.029	.049	.071	.131	.20	.34	.45
3	.00002	.00015	.0011	.0033	.0071	.013	.033	.065	.15	.24
4			.00007	.00029	.00083	.0018	.0067	.017	.058	.11
5				.00002	.00008	.00021	.0011	.0037	.018	.042
6				<.00001	.00001	.00002	.00014	.00061	.0044	.013
7					<.00001	<.00001	.00001	.00007	.00077	.003
8									.00007	.0003
n = 10										
2	.0016	.0061	.022	.044	.072	.102	.18	.27	.43	.54
3	.00004	.00031	.0022	.0063	.013	.023	.057	.10	.23	.33
4		.00001	.00018	.00076	.0021	.0044	.015	.036	.11	.18
5			.0001	.0008	.00028	.00072	.0035	.011	.043	.091
6				.00001	.00003	.00010	.00067	.0026	.015	.040
7						.00001	.00010	.00054	.0046	.015
8							.00001	.00009	.0011	.0043
9								.00001	.00019	.00099
10									.00002	.0001

* Numbers in the body of the table represent a priori probability levels chosen. Numbers in the left column under each group size signify the number of subjects that must have activation in a given brain voxel to reach the level of chosen significance in the table. Tables can be constructed for all group sizes.

1998], both of which peaked between 2–5 min after the completion of the drug injection.

Regions of significant drug effect were determined based upon combined treatment effect groups. From Table I (for n = 10; saline "hit" rate = .03), it can be seen that if the same voxel was activated in 5 of 10 subjects, it was significantly different than what would be expected after saline at a $P < 0.0008$ level. Representative views of the activation map from the nicotine treatment are shown in Figure 5. Only those voxels that passed both the WAP analysis and the statistical criteria above are illustrated. It can be seen that there is extensive activation after 1.5 mg of nicotine including regions of the cingulate cortex, inferior, medial and superior frontal gyri, insular cortex, angular gyrus, and cuneus. In addition, there was activation in the putamen, hypothalamus, and amygdala. No areas were significantly activated after saline.

DISCUSSION AND CONCLUSIONS

The waveform analysis methodology described above for the detection of drug-induced changes in fMRI signal has enabled us to map and quantify in a rigorous manner, the effects of a psychoactive drug in the human brain. The effectiveness of the method is demonstrated in that it detects discrete areas of activation that are generally consistent with the localization of nicotinic receptors in the brain [Nyback et al., 1989] and the known pharmacological action of nicotine [Henningfield et al., 1995]. In addition, our detection algorithm is based upon the published plasma pharmacokinetics of the drug [Benowitz et al., 1990; Stein et al., 1998], the time course of behavioral effects produced by iv nicotine and the general pharmacokinetic model for a drug effect. This methodology makes use of much more of the information in the fMRI waveform than the only other technique that has been proposed for the detection of drug-induced fMRI signal changes [Breiter et al., 1997], which uses the Kolmogorov-Smirnov two-sample test [Siegel, 1956] to detect differences in signal intensity before and after drug injection. Whereas this latter method is being successfully used, it makes no assumption of drug effect, provides no information on time of onset or duration of effect, and little information regarding effect magnitude.

The statistical model for the probability of observing multiple voxels depends upon two assumptions: that data between subjects are independent and that the distribution of the proportion of activated voxels

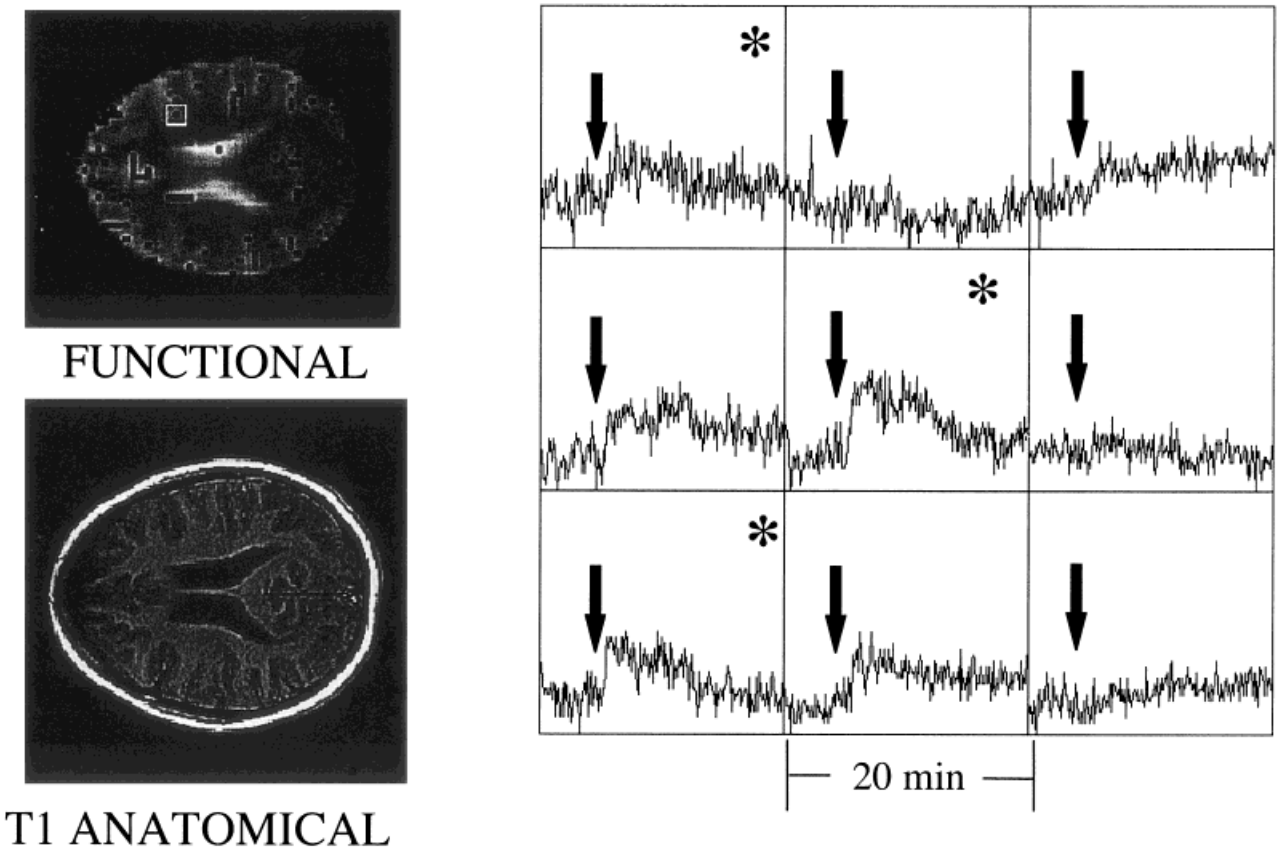

Figure 4.

fMRI time course data from a representative subject following the iv injection of 1.5 mg of nicotine. Shown are the echoplanar (EPI) functional image and its corresponding T1 weighted fast spin echo anatomic image. The black pixels on the functional image represent those voxels passing the WAP analysis for nicotine effects. The white box on the functional image shows the 3 × 3 voxel region corresponding to the time course data illustrated on the right side of the figure. Each time course graph illustrates the EPI signal plotted against time for the nine contiguous voxels (each voxel is 3.75 mm^2) encompassed by the box. Individual data points were acquired every 6 sec during the 20-min acquisition period resulting in 200 measurements for each voxel. The arrows indicate the time of injection onset. Note that the three voxels indicated by (*) passed the WAP criteria and are seen as dark areas in the corresponding positions in the functional image.

between subjects can be adequately modeled by the beta distribution. The first assumption holds unless one is repeatedly imaging the same person instead of multiple individuals. The second assumption depends upon the flexibility of the beta distribution, which is a very flexible distribution and will be matched by the observed sample mean and standard deviation. It will always distribute its probability across the entire range of probabilities (0–1) and thus will be slightly conservative when the data is unimodal (i.e., has a single peak). In contrast, if the observed reference probabilities are bimodal (two peaks that might indicate two different subject groups), it may be more liberal than it should be.

Each voxel is tested separately compared to a reference that has randomly activated voxels. For maximum sensitivity, α and β should be fit to the observed reference data using maximum likelihood; however, we found with our data that using the moment estimates for α and β produced an adequate indexing of the beta distribution. In addition, increased ability to reject false positives is accomplished by using a clustering criterion. For our data we did not observe any clusters in the saline infused data; however, this clearly depends on the initial type one statistical error chosen. A choice of 1% is 4.9 times less likely to produce chance clusters than a choice of a 5% criterion for false positives.

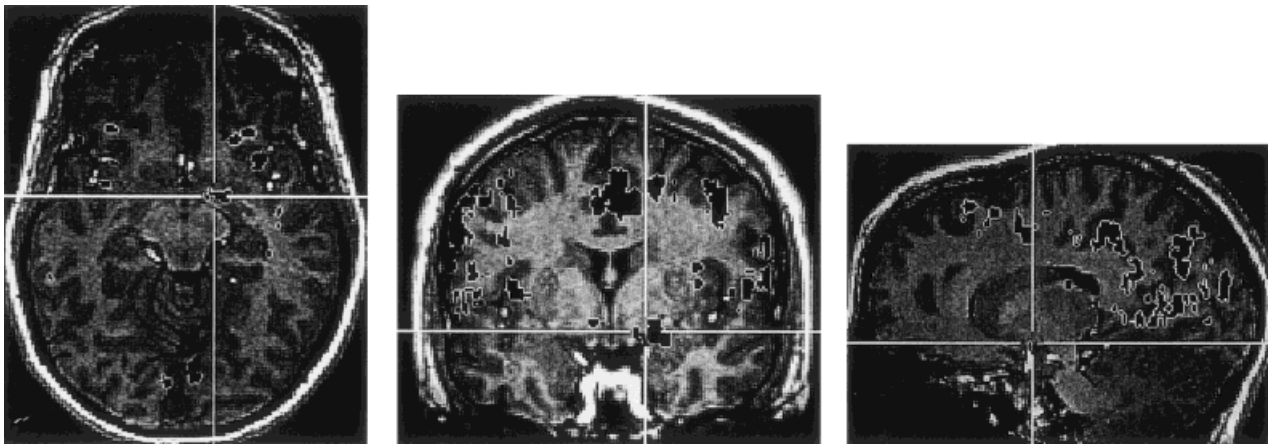

Figure 5.
Composite 3D fMRI images averaged across all subjects indicating areas of statistically significant ($P \leq 0.0001$) activation by 1.5 mg iv nicotine. The composite functional images are superimposed upon a single subject's Spoiled GRASS anatomical data set. The blackened pixels show the areas of significant drug-induced activation.

The general WAP methodology allows for the setting of the sensitivity and specificity for individual voxels. By adjusting the criteria for parameters, the number of false positives can be adjusted. Since the method includes a simple t-test for the base line versus the peak, by setting the criteria to follow the pharmacological response curve, one can increase sensitivity over the t-test without any loss of power (with a t-test, there is a direct tradeoff) by estimating false positives that could not be a pharmacological response while retaining all potential pharmacological responses. For example, the following three systematic errors would be called significant by t-test, even if one adjusted for the autocorrelation among successive fMRI measurements: (1) a gradual drift in the signal often seen in fMRI over time would be rejected because the rate of increase is too slow and there is no downturn, (2) an abrupt jump in the background would be rejected by this method because it has too rapid an increase and again no decrease, and (3) a square wave would be rejected because it has neither a correct rise nor fall time. Notably, any of these could have had a significant t-test.

Another important issue is using the correct probabilities across subjects to make correct inferences and the effect of multiple tests of significance on each voxel. The multiple testing problem is the number of false positives induced by a test with significance level alpha applied to thousands of voxels. This is entirely different from the multiple comparisons problem that involves comparisons of every pair (n^2) of voxels. The solution to this problem is to reduce the number of false positives compared to true positives. The false positive level can be reduced by arbitrarily choosing a smaller alpha level with a concomitant reduction in power, increasing the stringency of the WAP criteria, which will result in a much smaller reduction in power since the test is now eliminating more of the voxels whose random fluctuations mimic the drug's time-effect curve, and / or by adding a clustering option that, by excluding isolated voxels, reduces the number of false positives with a minimal if any effect on the power. Clustering algorithms [Friston et al., 1994; Forman et al., 1995] give the greatest ability to decrease the number of false positive tests without losing power to detect aggregate clusters of activated voxels, which may be the only pharmacologically meaningful result.

The rigor of this method may more likely lead to the rejection of some drug-induced brain effects rather than provide a high number of false positives. Any drug effect that does not follow the pharmacokinetic model described above will be rejected. Thus brain areas that respond to nicotine with decreased activity or highly sustained activation beyond the expected period will not be detected. It should be pointed out, however, that such waveforms are not precluded from detection, as WAP permits an analysis of negative going waveforms as well a those with longer $T_{1/2}$ values. Comparisons between doses is also possible if the mean percentage of voxels activated by one of the doses is sufficiently low. The WAP protocol also accepts as activated, a small percentage of voxels result-

ing from the saline treatment. This may be a result of random variations in the MR signal appearing in a few of the millions of voxels evaluated or as a result of correlated head motion. This interpretation is supported by the fact that these ''activated'' voxels appear to be randomly distributed in the brain and not localized or clustered together to form distinct regions of activation. Indeed, we found no instances where the same voxel was significantly activated in five or more subjects after saline, as opposed to the nicotine data. Alternatively, punctate brain areas may be responding to nonspecific factors associated with the injection and / or imaging protocol.

The pharmacological relevance of the areas where nicotine-induced activation was detected using the proposed method is supported by studies of nicotinic receptor binding as well as the known pharmacological action of nicotine in humans. The localization of nicotinic receptors in the human brain has been studied using PET imaging [Nyback et al., 1989]. High levels of receptors were observed in frontal cortex, insular cortex, and cingulate. This distribution agrees well with the activation observed in the present study. We also observed activation in several additional subcortical brain regions such as the amygdala, nucleus accumbens, hypothalamus, and thalamus that have not been previously identified by PET imaging. This may be due to both the increased temporal and spatial resolution of fMRI and the technique's sensitivity to activation in areas receiving the output from neurons having nicotinic receptors. Taken as a whole, the congruence of the pharmacokinetic, behavioral, and time course data support our contention that the changes in fMRI signal detected by WAP reflect drug induced alterations in neuronal activity.

In conclusion, we have presented a pharmacologically based waveform analysis protocol for the extraction and analysis of changes in fMRI signal induced by psychoactive drugs and have demonstrated its effectiveness by analyzing an acquired data set. This analysis paradigm is still incomplete in that it may not extract all biologically relevant effects of a particular drug. Future studies are planned to examine regional differences in onset and offset of drug effects. Additional detection algorithms must be developed as more is learned about the physiological and biophysical basis of the BOLD signal and the interactions of pharmacological agents on this signal and other pulse sequences weighted toward blood flow. Nevertheless, those voxels that are identified after IV drug administration and meet the rigorous criteria outlined, accurately reflect drug-induced brain activity patterns that are consistent with the known neuroanatomy, pharmacology, and behavioral effects of nicotine in humans.

ACKNOWLEDGMENTS

This work was supported in part by USPHS grant DA09465 to E.A.S.

REFERENCES

Bandettini PA, Jesmanowicz A, Wong EC, Hyde JC. 1993. Processing strategies for time-course data sets in functional MRI of the human brain. Magn Reson Med 30:161–173.

Benowitz NL, Porchet H, Jacob PI. 1990. Pharmacokinetics, Metabolism and Pharmacodynamics of Nicotine. Oxford: Oxford University Press.

Binder JR, Rao SM, Hammeke TA, Frost JA, Bandettini PA, Hyde JS. 1994. Effects of stimulus rate on signal response during functional magnetic resonance imaging of human auditory cortex. Cogn Brain Res 2:31–38.

Breiter HC, Gollub RL, Weisskoff RM, Kennedy DN, Makris N, Berke JD, Goodman JM, Kantor HL, Gastfriend DR, Riorden JP, Mathew RT, Rosen BR, Hyman SE. 1997. Acute effects of cocaine on human brain activity and emotion. Neuron 19:591–611.

Cox RW. 1996. AFNI: software for the analysis and visualization of functional magnetic resonance images. Comput Biomed Res 29:162–173.

DeYoe EA, Carman GJ, Bandettini P, Glickman S, Wieser J, Cox R, Miller D, Neitz J. 1996. Mapping striate and extrastriate visual areas in human cerebral cortex. Proc Natl Acad Sci USA 93:2382–2386.

Evans M, Hastings N, Peacock B. 1993. Statistical distributions. New York: John Wiley & Sons.

Forman SD, Cohen JD, Fitzgerald M, Eddy WF, Mintun MA, Noll DC. 1995. Improved assessment of significant activation in functional magnetic resonance imaging (fMRI): use of a cluster-size threshold. Magn Reson Med 33:636–647.

Friston KJ, Worsley KJ, Frackowiak RSJ, Mazziotta JC, Evans AC. 1994. Assessing the significance of focal activations using their spatial extent. Hum Brain Mapp 1:214–220.

Hardman JG, Limbird LE. 1996. Goodman & Gilman's The Pharmacological Basis of Therapeutics. New York: McGraw-Hill.

Henningfield JE, Schuh LM, Jarvik MJ. 1995. Pathophysiology of tobacco dependence. In: Bloom FE, Kupfer DJ (eds): Psychopharmacology: The Fourth Generation of Progress. New York: Raven Press, pp 1715–1726.

Milliken GA, Johnson DE. 1992. Analysis of Messy Data. New York: Chapman-Hall.

Nyback H, Norberg A, Langstrom B, Halldin C, Hartvig P, Halin A, Swahn C-G, Sedvall G. 1989. Attempt to visualize nicotine receptors in the brain of monkey and man by positron emission tomography. Progress Brain Res 79:313–319.

Ogawa S, Lee TM, Kay AR, Tank DW. 1992a. Magnetic resonance imaging with contrast dependent on blood oxygenation. Proc Natl Acad Sci USA 87:9868–9872.

Ogawa S, Menon RS, Tank DW, Kim SG, Merkle H, Ellerman JM, Ugurbli K. 1993. Functional brain mapping by blood oxygenation level-dependent contrast magnetic resonance imaging: a comparison of signal characteristics with biophysical model. Biophys J 64:803–812.

Ogawa S, Tank DW, Menon R. 1992b. Intrinsic signal changes accompanying sensory stimulation: functional brain mapping resonance imaging. Proc Natl Acad Sci USA 89:5951–5955.

Siegel S. 1956. Nonparametric Statistics for the Behavioral Sciences. New York: McGraw-Hill.

Sokoloff L. 1977. Relation between physiological function and energy metabolism in the central nervous system. J Neurochem 29:13–26.

Stein EA, Pankiewicz J, Harsch HH, Cho JK, Fuller SA, Hoffmann RG, Hawkins M, Rao SM, Bandettini PA, Bloom A. 1998. Nicotine-induced limbic cortical activation in the human brain: a functional MRI study. Am J Psychiatry 155:1009–1015.

Talairach J, Tournoux P. 1988. Co-planar Sterotaxic Atlas of the Human Brain. New York: Thieme.

Wong EC, Boskamp E, Hyde JS. 1992. A volume optimized quadrature elliptical endcap birdcage brain coil. 11th ann Sci Mtg Soc Magn Reson 105.